Sheffield Hallam University

An investigation to establish the source of the Roman lime mortars used in Wallsend, UK

LAYCOCK, Elizabeth <http://orcid.org/0000-0003-3758-6829>, PIRRIE, Duncan, CLEGG, Francis <http://orcid.org/0000-0002-9566-5739>, BELL, Anthony and BIDWELL, Paul

Published version

Copyright and re-use policy

An investigation to establish the source of the Roman lime mortars used in Wallsend, UK

AUTHOR

Laycock, Elizabeth Anne [a] Pirrie, Duncan [b], Clegg, Francis [a] Bell, Anthony Martin Thomas [a], & Bidwell, Paul [c]

Affiliations

a. Sheffield Hallam University, Howard Street, Sheffield, S1 1WB E.A.Laycock@shu.ac.uk
b University of South Wales, School of Applied Sciences, University of South Wales, Pontypridd, Wales, CF37 4BD
c 8 Dockwray Square, North Shields, NE30 1JZ

Corresponding Author **Laycock, Elizabeth Anne**
+44114 225 3200
Howard Street, Sheffield, S1 1WB E.A.Laycock@shu.ac.uk

Abstract

This paper presents the results of analytical work which aimed to explore potential sources for the lime mortar used in the Hadrianic fort baths and a third-century repair to Hadrian's Wall at Wallsend, UK. It is generally assumed that quick lime for mortar is produced close to the source, however, as yet, no archaeological evidence of kilns has been found in the Wallsend area. After extensive analysis the mortars were found to be very different in characteristics and suggest variable sources for the quarried limestone and for the aggregates used to manufacture the mortar. Precedence exists in other locations for quicklime to be sourced from kilns set at some considerable distance from Roman construction sites.   It is only at Housesteads and Vindolanda, sited close to Carboniferous Limestone outcrops, that Roman lime kilns have been discovered to date. Therefore the investigation included a number of potential sources in the vicinity of Housesteads as well as Permian limestones at Trow Point which is geographically the closest source of limestone.   Results suggest that Carboniferous limestone was the most likely source for some of the mortars analysed which may suggest that areas for lime production
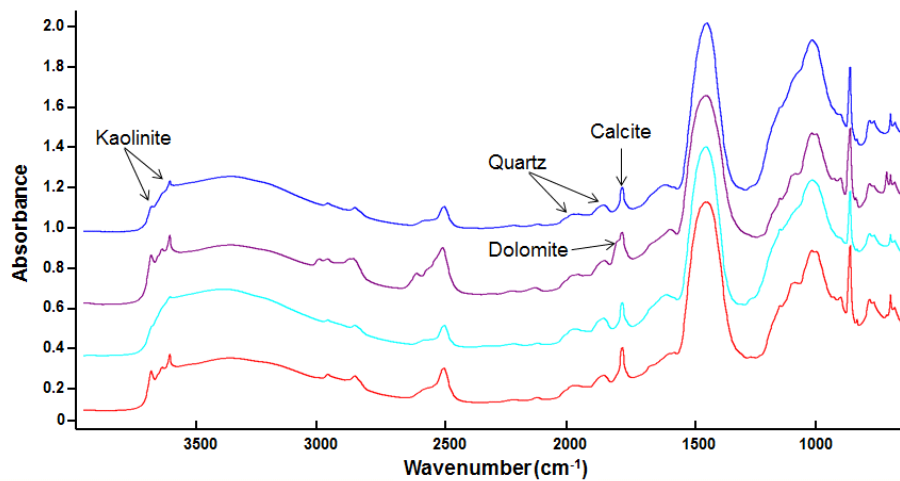
are less numerous than previously thought and may even have been concentrated around one area.

Keywords

limestone; mortar; Roman; petrography; XRD, FTIR

Graphical Abstract
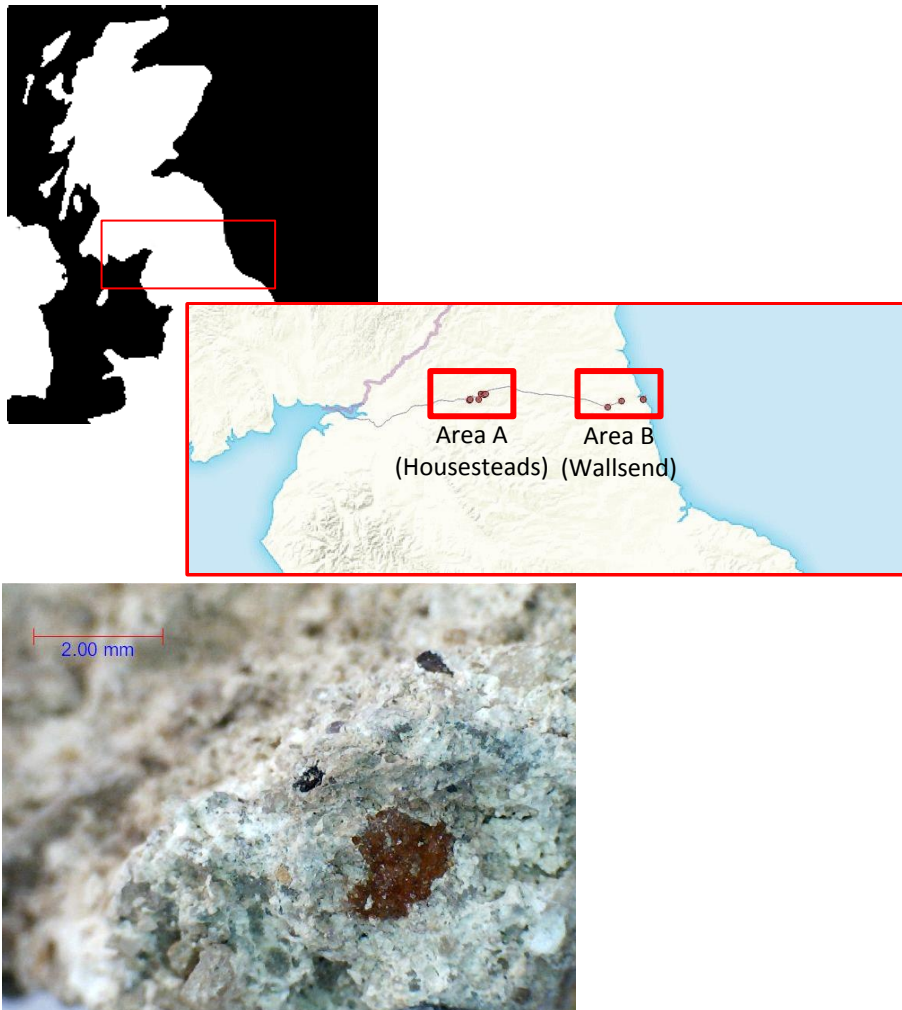
Highlights

- Mortar characteristics (binder type and ratio, grading) were different

- Most likely source rocks are the calcareous Carboniferous limestones

- The automatic assumption of the most local source of lime for mortar is challenged

Introduction

Hadrian's Wall is a designated UNESCO World Heritage site and consists not only of the wall itself, but the milecastles, forts and associated temples. It is the most elaborate of the fortifications enclosing parts of the Roman Empire. Much of the archaeological investigations to date have focused on the forts, milecastles and turrets. Archaeological work at Wallsend (Bidwell, 2018) provided the opportunity to analyse recovered lime mortar samples from Hadrians Wall and from the nearby baths built at the same time. While lime mortar was not used in the original construction of Hadrians Wall it was extensively used in the fort and baths as well as in later repairs to the wall itself. As there are no outcrops of limestone in the immediate vicinity of Wallsend, the source of the mortar is uncertain. Consequently, a range of analytical techniques were used to characterise the mortar and potential limestone source materials, to explore the question of the mortar provenance.

Background

Hadrian's Wall was built as a frontier between the Roman Empire's province of Britannia and the territories of the Iron Age peoples to the north. Initial building started in AD 122 and lasted about a decade. The wall averaged 4 m high and 3 m wide and required the placing of an estimated 30 million facing stones (Gillette, 2000), as part of the estimated 3,713,000 tonnes of bulk building materials (facing and core stone, clay and timber) required for the whole wall (Kendal 1996). There are ongoing archaeological investigations studying many aspects of the construction details and life on the wall but still many fundamental unknowns. The source of much of the building material is still uncertain, although recent work by Allison (2015) using GIS (geographical information system) modelling identified potential stone types and Roman building stone quarries with legionary inscriptions and their distances from the wall or from other structures. These locations varied from as little as 300 m from the wall to as much as 34 km with a median value of 5 km. The initial construction of the 'Broad Wall' generally had a clay and rubble core, with a poor brown mortar used in some places for the facing stones (Symonds & Mason, 2009). The eastern end of the wall was extended from Newcastle to Wallsend a few years after the construction of the main wall had commenced. This was part of the "Narrow Wall," representing a second stage in the building programme when the original specification for the "Broad Wall" had been abandoned. The source of the mortar used in the construction of the "Narrow Wall" and later phases of construction is unknown. As Hodgson (2006) stresses, the building activity on the wall was not always driven by political events but by social-historical factors which

are considerably more complex. Recent thinking suggests that the building programme was altered to in order to complete the work as quickly as possible, not least because of the direct involvement of the emperor Hadrian.

There are structures surviving in the regions of the central and east walls arising from lime burning activities of the 18th and 19th Centuries. While the practice of quicklime production was certainly carried out in the late 15th and early 16th centuries as well as by the Romans (Carlton et al. 2011), surviving kilns from the Roman period within the vicinity of Hadrian's wall are relatively rare. A Roman lime kiln on a limestone outcrop is suggested at Queens Crags which is 800 metres north of Sewingshields Crags near Housesteads (Crow, 1991), another was identified in the area between the eastern fort ramparts of Housesteads and the Knag Burn (Simpson 1976), the latter is the only excavated example known from the line of the wall (Symonds & Mason, 2009). These are however, a significant distance from Wallsend. The only two Roman lime kilns so far encountered in the wall zone are at Housesteads and Vindolanda, the first dug in 1909 with the kiln at Vindolanda, found in 1995 but not fully published. There are two mentions of lime in the Vindolanda writing-tablets, one in a roster which listed "19(?) men 'burning stone'" (Bowman & Thomas, 1994 TV II,156.4) and the other a letter about carts and an order for lime (Bowman & Thomas, 1994, TV II, 314.2). Both are of Period 3 (97–102/3), well before the start of the building of the wall, and presumably to do with the building of the bath-house which is currently the only known stone building of that period at this site. When work started on the wall, sources of limestone were already known and had been exploited in the Housesteads/ Vindolanda area.

The assumption of Kendal (1996) was that much of the transport of raw materials would be facilitated overland – however, Crocker and Oliver (1999 cited by Allison 2015) suggested that even relatively narrow water courses, less than 2 m wide, were used for moving heavy materials, such as stone in the Medieval period. Therefore the use of water transport should not be discounted in the Roman period especially given the distances over which building stone was transported to the wall (Allison, 2015).

Lime for mortar is generally produced where limestone and a source of fuel were readily available. The majority of excavated Roman lime kilns are of the 'periodic' type where a timber formwork was constructed onto an internal shelf within the furnace in order to provide support for the limestone charge. This formwork provided initial support over the fire in the kiln chamber (Dix, 1982). As this frame burnt away the charge became self-supporting allowing ash to be removed before unloading, preventing contamination from the ashes in the bottom of the kiln. Clamp kilns were also used, and remains have been suggested at several Roman sites (Dix, 1982 cited Wheeler & Wheeler 1936; Pitt-Rivers 1887; Bushe-Fox 1932, Liversidge et al. 1987 and Neal 1974). The clamp kilns produced quicklime which was mixed with the fuel ash and was not as evenly burnt (calcined) as that from the periodic kiln. Periodic kilns are believed to be less efficient in terms of fuel requirements (Thér & Maršálek, 2013), but capable of more effective conversion to quicklime. If the kilns used to produce the lime of Hadrian's wall were fired periodically and were of a similar size to those of the legionary lime-plant at Iversheim (5.5 m^3) then a kiln could be expected to produce 40 tonnes of lime each month Dix (1982). Kendal (1996) interpolates that the whole wall would therefore

require between 12 and 15 kilns. If timber was used as the fuel for firing (as well as for structural uses on the wall and scaffolding) then an estimated 250 ha of woodland would need to be cleared along the length of the wall with the largest requirement for lime burning (Kendal, 1996). Indeed, Dumayne (1994) shows that the changes in pollen deposited in Fozy Moss between 129AD and 370AD are consistent with extensive deforestation.

After firing there would be some limestone which was unburnt, this could be removed during slaking. The presence of unburnt limestone was confirmed in field archaeology experiments by Thér & Maršálek (2013) and Storemyr (2017). In each case the use of sub-optimal wood was cited as resulting in material which was partially 'burnt' (calcined) or uncalcined in each charge. Storemyr (2017) also demonstrated the changes in colour which could occur with fluctuating raw material properties and contamination due to vault collapse during firing.

In order to evaluate the mortar an appraisal of the literature was carried out. A selection of the references which informed the study are summarised in Table 1. From this it can be seen that past studies on historic mortars utilise a variety of different methods. The most commonly used being that of optical study at a variety of scales (in hand specimen, by binocular or polarising microscope) and XRD. Some studies also use TGA/DSC and ICP-OES/AES, which were not used in this work. The decision was made to undertake a selection of the methods outlined by Middendorf et al. (1999) as summarised in Figures 1a to 1c.

Materials and Methods

Authors	Mortar description /location	Characterisation Method.									
		●	⊕	♦	⌗	■	✧	•	⊞	★	□
This study	Mortars from Wallsend, UK	●	⊕	♦	⌗	■	✧	•	⊞	★	□
Moropoulou et al (1995)	Ancient, Byzantine and later mortars						✧	•			
Böhm (2000)	19th Century hydraulic mortars	●	⊕	♦	⌗		✧	•		★	
Middedorf, et al (2000)	Old mortars		⊕	♦	⌗	■	✧	•	⊞	★	
Moropoulou et al (2000)	Byzantine mortars		⊕				✧	•	⊞	★	□
Maravelaki-Kalaitzaki et al. (2003)	Ancient Cretan Mortars		⊕	♦			✧		⊞		
Silva et al (2005)	Roman Colosseum and cistern.		⊕				✧	•	⊞		
Genestar et al. (2006)	Ancient mortars from Roman Pollentia (Spain)			♦			✧		⊞	★	
Velosa et al (2007)	Roman mortars from Conímbriga, Portugal	●	⊕			■	✧			★	
Zambaet al (2007)	1st century AD mortars of Saithidai Heroon Podium (Messene Peloponnesus, Greece)						✧	•			
Franquelo, et al.(2008)	Roman cermanic sof hydraulic mortar. Mithraeum of Merida (Spain)					■	✧	•		★	□
Pavia & Caro (2008).	Roman mortar, La Rioja, Spain		⊕								
Özkaya & Böke (2009)	Roman mortars Serapis temple, Pergamon			♦			✧	•			□
Coroado et al. (2010)	Traditional lime mortars (Portugal)					■	✧			★	□
Robador et al (2010)	Roman Mithraeum house in Augusta emerita, Spain		⊕	♦		■	✧		⊞	★	
Šagm et al (2012)	Roman buildings in Nysa and Aigai,Turkey						✧	•	⊞	★	
Drdácký et al. (2013)	Roman mortars Ponte di Augusto (Italy)	●	⊕					•			□
Gulza et al. (2013)	Mortars from Jahangir Tomb (Pakistan)		⊕				✧	•	⊞		□
Papayianni et al (2013)	Roman Odeion at Dion	●								★	□
Yaseen et al (2013)	Roman mortars from Jerash, Jordan		⊕			■	✧	•			
Pires, J (2014)	Historical Lime	●		♦			✧		⊞		
Leone et al. (2016)	Mortars from Herculaneum (Italy)	●	⊕	♦		■	✧		⊞		

Table 1 Summary of methods used in previous studies of ancient mortars.

Key: Macroscopic (Hand specimen, binocular microscope)(●); Optical microscopy (polarising light)(⊕); HCl dissolution (♦); Sodium carbonate dissolution(⌗); XRF (■); XRD (✧); SEM (•); FTIR (⊞); Grain size distribution of aggregate (★); porosity / MIP (□)
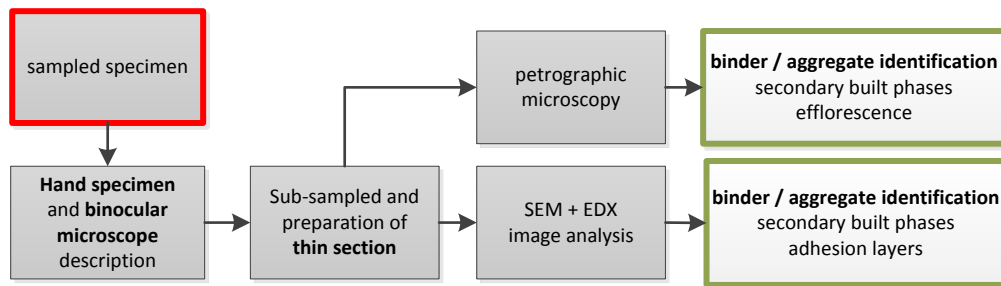
Figure 1a Flow chart of mortar tests used in this work (modified after Middendorf et al 1999). Shaded boxes indicate methods used. Green bordered boxes are the outcomes of the tests
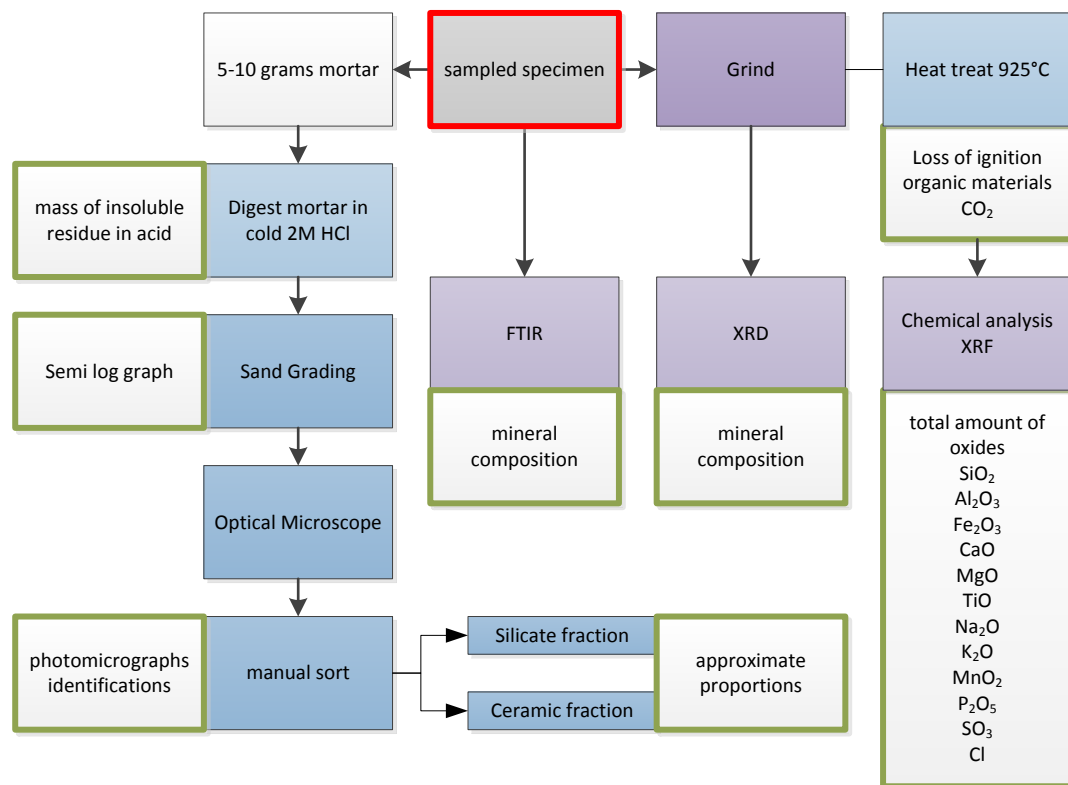

Figure 1b Flow chart of mortar tests used in this work (modified after Middendorf et al 1999) Shaded boxes indicate methods used. Green bordered boxes are the outcomes of the tests
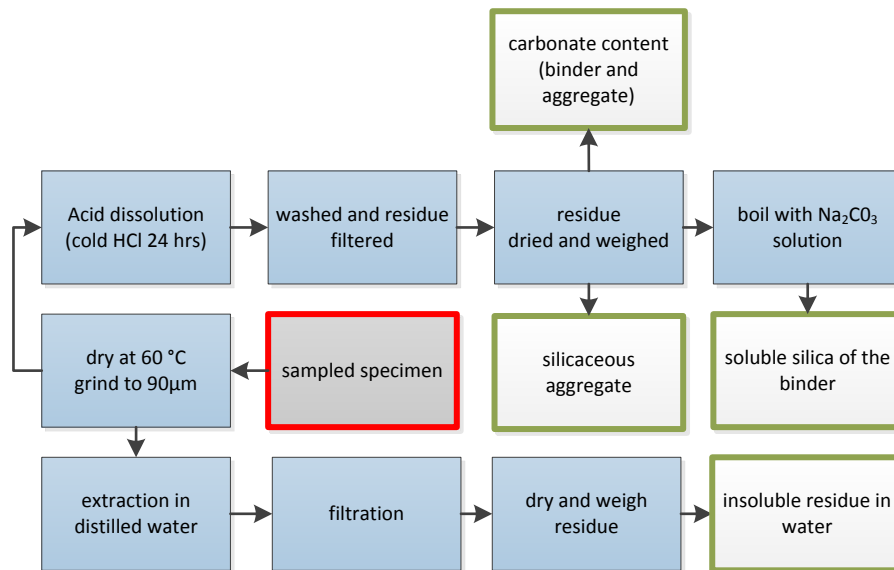
Figure 1c Flow chart of mortar tests used in this work (modified after Middendorf et al 1999). Shaded boxes indicate methods used. Green bordered boxes are the outcomes of the tests

Samples of mortar for testing

Four samples of mortar were provided by Paul Bidwell for analysis (Table 2). The two samples from Hadrian's Wall were from one of several third-century rebuildings, but it was the only one in which mortar was used. The baths were the only Hadrianic building at Wallsend available for sampling where mortar was used; one sample was from the original construction, and the other, selected as a comparison to the mortared repair of the Wall, was from a partial rebuilding in the third century.

Sample code	Description	Location
WESH 1625	Hadrianic wall	Wallsend baths
WESH 1660	Used in build of SW flue, 3rd century	Wallsend baths
WBMT 8076	Repairs to Hadrian's Wall	Wallsend
WBMT 8083	Repairs to Hadrian's Wall	Wallsend

Table 2 Mortar samples and locations

Analytical methods

The four mortar samples were digitally photographed and then described in hand specimen after macroscopic identification (as used by Anderson et al. 2000) following the flow of procedures indicated in Figure 1a. The mortar samples were

then examined using binocular microscopy and then subsampled. The friable nature of the mortar samples required preparation as resin impregnated polished thin section. In total 9 thin sections (at least two from each) were prepared from the 4 samples submitted for examination.   The thin sections were petrographically analysed (as Drdácký et al. 2013) using transmitted light microscopy and imaged. The petrographic description followed Ingham (2011).

A dissolution methodology was used to segregate the aggregate fraction for sieve analysis from a whole sample of mortar (Figure 1b). Cold 2M HCl was used for 24 hours to dissolve the binder from the aggregate in case of the presence of an unknown fraction of Fe, Al and hydraulic silicates contained within the binding fraction which are sensitive to the hot HCl method (Alvares et al. 1999; 2000a; 2000b). After dissolution the clear solution was decanted and de-ionised water was used repeatedly to wash the residue free of chloride, these were then filtered and dried to constant mass. The resulting material was passed through a series of sieves to establish grading curves for the resulting non-carbonate aggregate fraction using 75 µm, 150 µm, 300 µm, 600 µm, 1.18 mm, 2.36 mm, 5.0 mm and 6.3 mm sieves.

To establish the acid soluble (carbonates) and soluble silica content of the mortar a quantity of the powdered sub sample was dried at 60°C to constant mass and was then added to HCl and then left for 24 hours (Figure 1c). The clear solution was decanted off and de-ionised water was used to wash the sample free of chloride with the washing procedure repeated several times. Samples were filtered and dried to constant mass to establish the weight loss and hence the carbonate fraction. To

establish the soluble silica content, the resulting filtrate was added to a saturated solution of Na_2CO_3, heated and held at boiling point for 5 minutes. This was then filtered through a weighed filter paper and the residue washed five times with hot deionised water, 5 times with hot diluted HCl (1:20) and a further five times with hot deionised water. Samples were dried at 60°C to constant mass.

To carry out X-Ray Fluorescence (XRF) (as Middendorf et al. 1999) mortar samples were ground to 300 µm. Then for all 4 mortars approximately 1 g of sample was mixed with approximately 10 g of lithium tetraborate ($Li_2B_2O_7$) flux, this flux was doped with 0.5% lithium iodide as an anti-cracking agent. These mixtures were fused at 1065°C using a Claisse LeNeo fused bead maker. XRF spectra were collected using a PANalytical MagiX PRO XRF spectrometer and a Rh anode X-ray source, Na was the lightest element detectable with this instrument. XRF data were analysed using PANalytical OXI software based on the methodology devised by Giles et al. (1995). X-ray Powder Diffraction (XRD) data were collected on the same powdered samples using a PANalytical X'Pert Pro X-ray powder diffractometer. This instrument was equipped with a graphite monochromator and an 'Xcelerator' area detector, Cu K_α X-rays were used (λ = 1.5405 Å), operating at 40 kV and 40 mA. The angular range of 5 to 100 °2θ was as collected using the X'Pert Data Collection software and XRD data were analysed using X'Pert Highscore Plus software and the International Centre for Diffraction Data powder diffraction file database to identify the components present.   Fourier transform infrared spectroscopy (FTIR) analysis was performed using a Thermo Nicolet Nexus spectrometer and a Graseby Specac 'Selector' DRIFTS accessory. The ground samples at 5 wt% were further ground with

KBr for 1 minute using a pestle and mortar. Spectra of sample and KBr mixtures were ratioed against that of KBr alone. Mercury porosimetry used a Thermo Scientific Pascal 240 Mercury porosimetry system working within a pressure range of 0.1 to 200 MPa to measure pore sizes between 15 and 0.0074 μm. Increase speed was 6 - 14 MPa/min, decrease speed 9 - 28 MPa/min, temperature 22°C. Scanning electron microscopy (SEM) used an FEI Quanta 650 SEM with tungsten electron source coupled with Oxford Instruments AZtec Energy Dispersive Spectroscopy (EDX) on broken fragments.

Potential sources of limestone for mortar production

The areas for sampling were in part determined by initial XRD and XRF results on the mortars which identified three binders of low magnesium content , which suggested two possible limestone sources should be considered.

1) The area around Housesteads (NY 7896 6879) Figure 2a, 2b

- Known area of Roman Lime kilns
- Near resources of fuel (timber / coal)
- Source of transport (road / water)
- Generally of low magnesium content

2) Trow Point (NZ 3836 6666) Figure 2a, 2c

- Close to end point use
- Source of transport as Roman stone extraction was often carried out at coastal areas (Allison, 2015)
- Near a source of transport (coast and river Tyne)
- Near resources of fuel (local and imported)
- Some areas of limestone at the locality have low magnesium content

There are abandoned quarry workings at Trow point from recent times which may have obliterated evidence of any earlier extraction or processing, so the lack of archaeological remains cannot be used to discount the area.
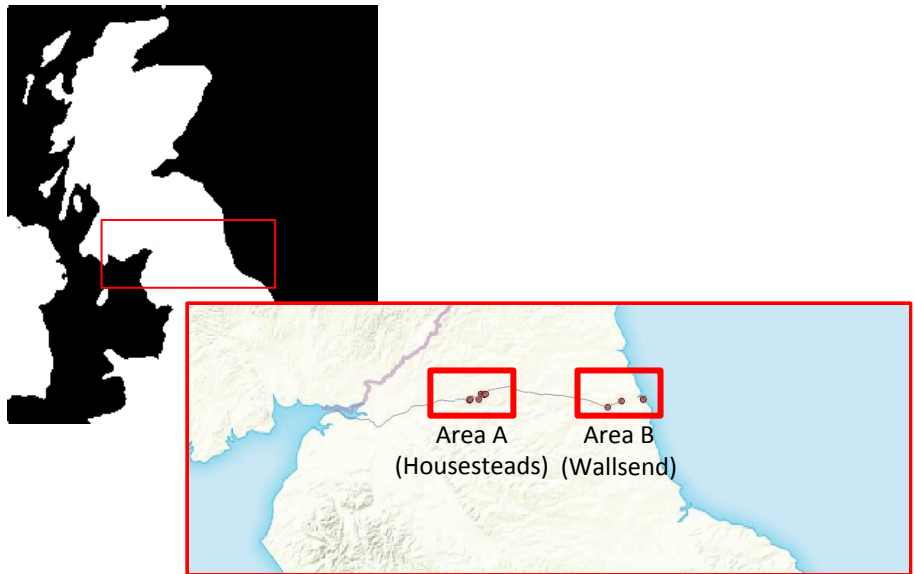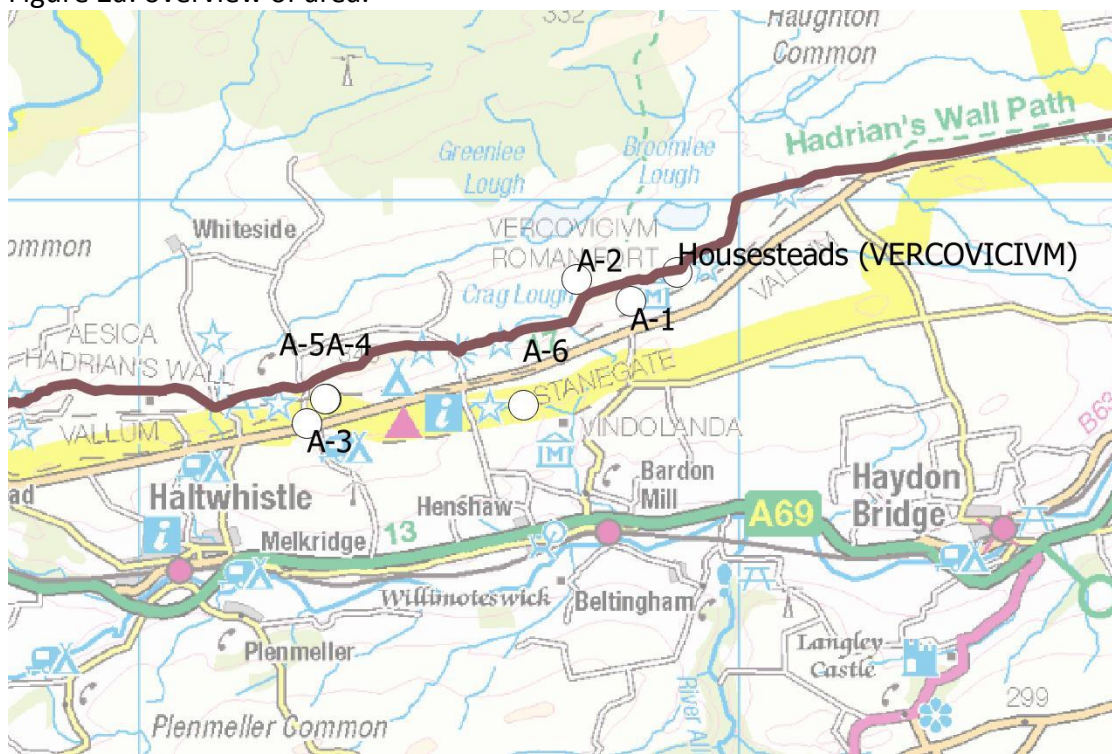
Figure 2a: overview of area.

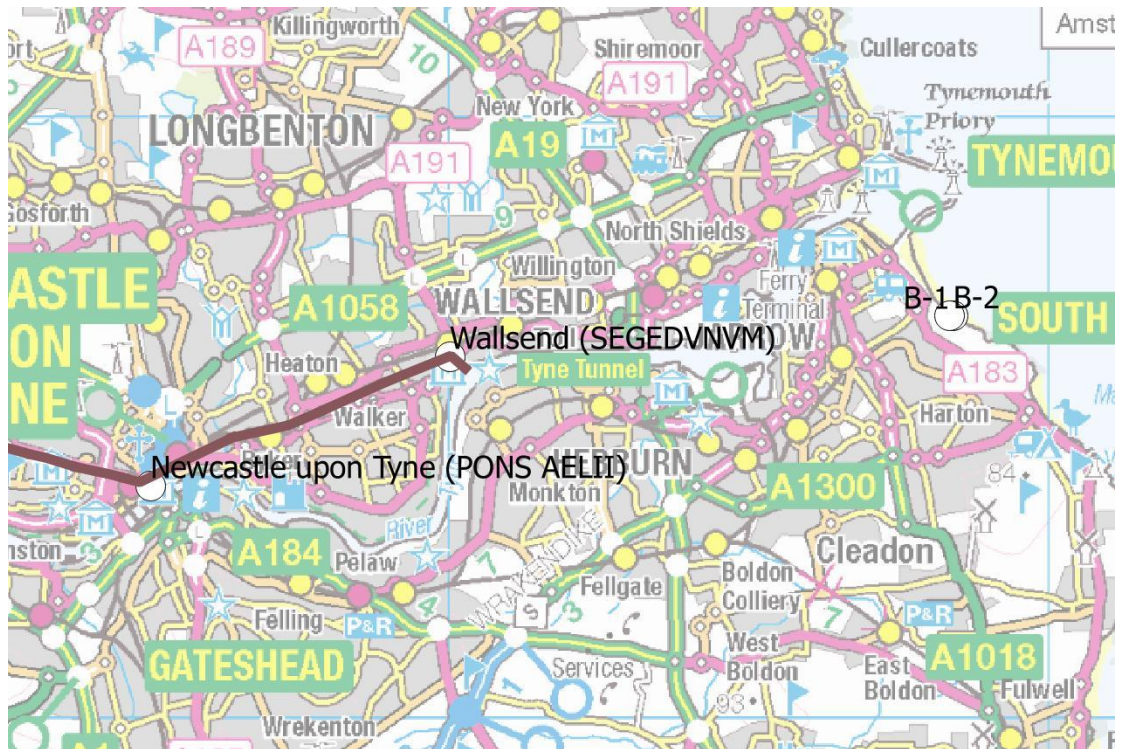Figure 2b Housesteads area (Area A.)

Figure 2c Wallsend (Area B)
Figure 2a 1:5,000,000 [TIFF geospatial data] Overview of Great Britian Updated: December 2014 Ordnance Survey Using: EDINA Digimap Ordnance Survey Service, http://digimap.edina.ac.uk/, Downloaded: November 2018 Ordnance Survey OpenData Licence
Figure 2b and 2c Map base: 1:250 000 Scale Colour Raster [TIFF geospatial data] Area around Haltwistle, Updated: June 2018, Ordnance Survey, Using: EDINA Digimap Ordnance Survey Service, http://digimap.edina.ac.uk/, Downloaded: November 2018 © Crown copyright and database rights 2018 Ordnance Survey
Figure 2c Map base: 1:250 000 Scale Colour Raster [TIFF geospatial data] Area around Newcastle-upon-Tyne, Updated: June 2018, Ordnance Survey, Using: EDINA Digimap Ordnance Survey Service, http://digimap.edina.ac.uk/, Downloaded: November 2018 © Crown copyright and database rights 2018 Ordnance Survey
Figure 2a, 2b and 2c Line of wall from Per Lineam Valli (2012)

The work of Harrison et al. (1990) gives chemical content for high purity limestones

considered to be strategic mineral resources, however the outcrops around

Housesteads are neither extensive nor pure enough to be included in this

assessment. Appropriate permissions to undertake sampling were therefore sought

as the land is owned by the National Trust, rented to private individuals and

additionally some sites were listed as a Site of Special Scientific Interest (SSSI) and

either Scheduled Monument or Special Area of Conservation. The relevant parties

were therefore English Nature, the National Trust, English Heritage and the individual tenants of the land (Table 3). The area around Trow Rocks is designated as an SSSI and is in the care of the National Trust again requiring appropriate permissions be sought (Table 3).

Schedule of sites sampled near Housesteads					
SET A	Grid Ref	Unit sampled	Listing status	Sheet no.	Group
A-1	NY782 683	Upper Bath House Wood / Scar	SSSI and SAM	19	UL
A-2	NY773 687	Colwell	SSSI and SAC	19	UL
A-3	NY728 663	Four Fathom		13	UL
A-4	NY731 667	Five Yard/ Eelwell	SSSI and SAM	13	UL
A-5	NY731 667	Great Limestone	SSSI and SAM	13	UL
A-6	NY764 666	Three Yard		13	UL
Schedule of sites sampled near Trow Point					
SET B		Unit sampled	Listing status	Sheet no.	Formation
B-1	NZ384 566	Raisby Formation	SSSI	21	Ra
B-2	NZ384 566	Concretionary Limestone Formation	SSSI	21	Ro

Table 3 Details of sample sites. SSSI – Site of special scientific interest. SAM – Scheduled monument. SAC – Special area of conservation. UL – Upper Liddesdale Group (Upper Carboniferous, Pendleian). Ra – Raisby Formation (formerly the Lower Magnesian Limestone). Ro – Roker Formation (formerly the Upper Magnesian Limestone).
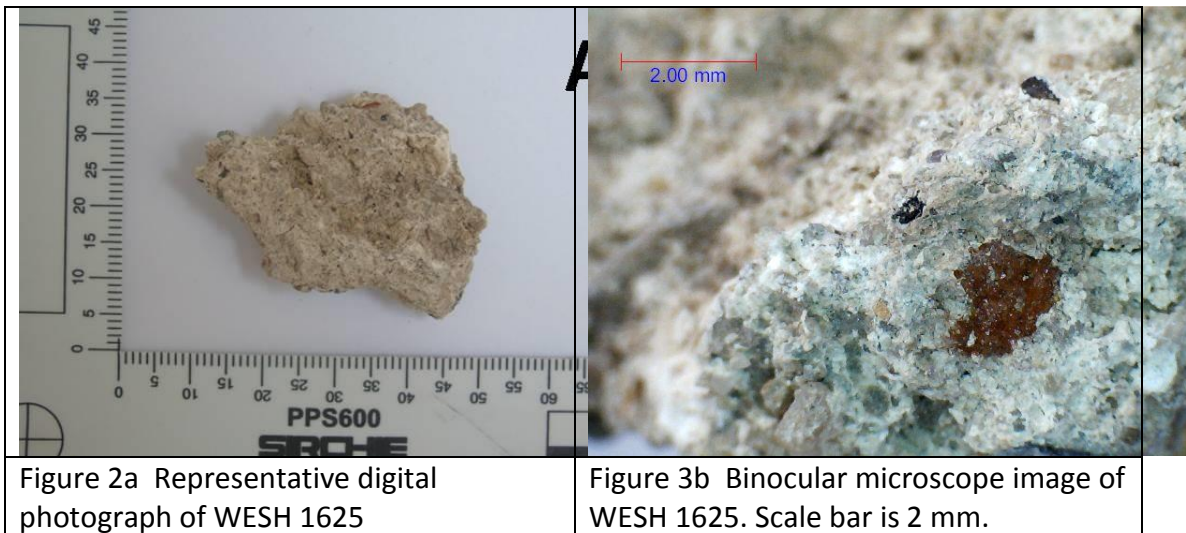
Results

Mortar analysis

Descriptions are provided for each sample in turn using hand specimen, binocular microscope and petrographic thin section techniques. Sample WESH 1625 was a pale grey (Munsell 10YR 8/2), highly porous, very soft, friable mortar. The aggregate size varied from very fine to coarse sand grade and was poorly sorted with darker, predominantly sub rounded / sub angular lithic clasts. Dominant aggregate grains comprised coarse sand grade grains of quartz, along with quartz-rich sandstones, dark grey rock fragments and red ceramic fragments (Figure 3). Under binocular

microscopy the sample was seen to be very porous, with pores commonly coated by secondary minerals. Dark grey angular fragments of limestone were present along with rounded quartz grains and clasts of quartz-rich sandstones and brick red/orange ceramic fragments were also present. The aggregate grains in the sample are markedly bimodal in size with sand-sized grains intermixed with particles typically ranging between 2 and 10 mm. The lime mortar appeared to be poorly mixed and in places had a "pelleted" texture. There were abundant shrinkage fractures throughout the mortar. The mortar has a very variable texture and microporosity throughout the section; the observed fractures are more abundant within some patches of the mortar than others. Within part of the section, there was a fibrous area, interpreted to have originally been plant material added to, or incorporated within, the mortar and in part replaced by carbonate. Petrographic analysis found that the sand grade aggregate grains were dominated by moderately well rounded quartz, with both plagioclase and K-feldspar, along with hornblende and also individual carbonate bioclast grains. A wide range of lithic grains made up the larger aggregate grains, but were predominantly composed of (a) quartz-rich sandstones and siltstones, (b) limestones, (c) dolerite/basalt and (d) clasts with a fine grained matrix interpreted to be fragments of man-made ceramics. Carbonate grain types present included: (a) muddy bioclastic limestones with foraminifera and echinoids, (b) bioclastic limestones in which the brachiopod bioclasts are replaced by Fe oxide hosted within a sparry calcite cement and (c) recrystallized limestones in which no primary fabric is retained and are probably dolomitised. Igneous grains present were composed of plagioclase laths, amphibole / pyroxene and opaques. The clasts were variable in grain size and are interpreted to be moderately fresh basalts /

dolerites. In addition to the lithic grains, particles interpreted to be man-made ceramics were also present. These grains are typically quite large (up to 10 mm) and were very fine grained (clay grade) with randomly oriented mica flakes.

| Figure 2a Representative digital photograph of WESH 1625 | Figure 3b Binocular microscope image of WESH 1625. Scale bar is 2 mm. |

Sample WESH 1660 was a pale grey (Munsell 10YR 8/2), soft, friable material with abundant pores with curved mineral coatings present on the pore margins. Aggregate grains were of quartz sand, dark grey rock fragments (possibly limestone) and red / orange-brown ceramic fragments. The aggregate was poorly sorted with angular to sub angular shape and predominantly of lithic origin with angular fragments of ceramic occurring throughout the grade range, and dominating the coarser fraction. On the surface of the sample were imprints of a fibrous material– possibly plant imprints, along with wood/charcoal (Figure 4). Under binocular microscopy abundant rounded medium-coarse grained quartz pieces were observed. Small fragments of orange/red/brick red ceramic were present along with shiny black grains of charcoal. The sample had a porous structure with a mammellar-like coating on the surface of the pores. Examined in thin section WESH 1660 had

abundant mortar with predominantly sand grade aggregate grains (less than 2 mm across). The aggregate fraction was dominated by sand-grade quartz, and grains composed of individual minerals include K feldspar, muscovite, hornblende and bioclasts. Small fragments of sandstone composed of quartz, biotite/muscovite mica and opaques were present along with quartz sandstones with carbonate cements. Carbonate grains present include individual echinoderm grains, recrystallized limestones and bioclastic limestone pieces. Some of the carbonate grains appeared to have reaction rims around their margins. In addition, partially dolomitised limestone clasts and siliceous particles of chert are also present. In addition to the naturally occurring mineral and rock grains present within the mortar there are also abundant pieces of charcoal. Fine grained (clay-rich) particles with dispersed quartz are also present and are interpreted to be man-made ceramics. In addition there is a large cellular particle which has been largely replaced or infilled by lime mortar and with the porosity infilled by resin. This particle was interpreted to be a relict area of fibrous plant material either added to, or incorporated within the mortar. The sample has abundant lime mortar with a fairly uniform appearance, although there do appear to be some small, patchy areas with apparently different density/microporosity. There are abundant shrinkage fractures present within the mortar, along with circular voids.
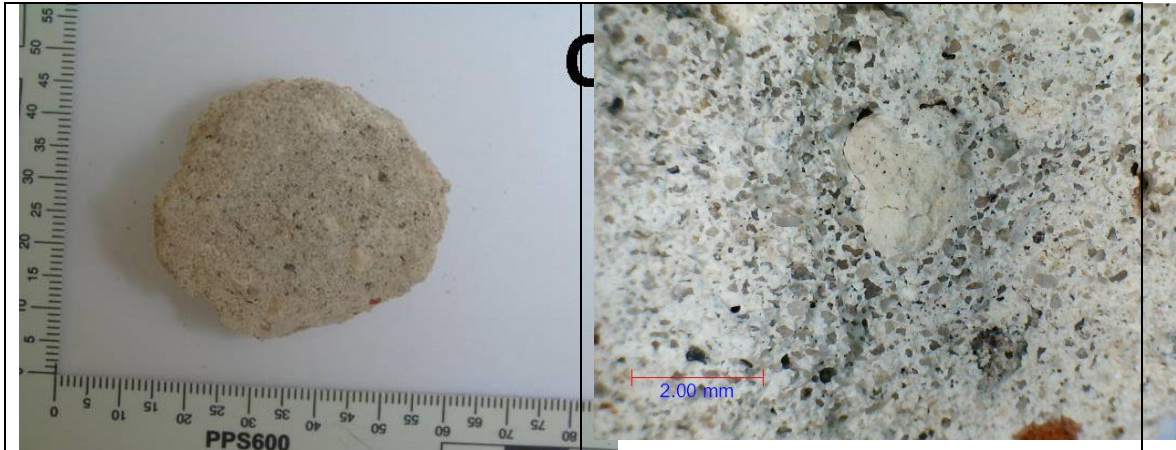
| Figure 4a. Representative digital photograph of WESH 1660 | Figure 4b. Binocular microscope image of WESH 1660. Scale bar is 2 mm. |

Sample WBMT 8076 was a pale grey (Munsell 10YR 8/2), soft, friable mortar sample. Aggregate was well sorted with angular to sub angular shape and predominantly of lithic origin with a trace amount of small angular fragments of ceramic (estimated <2%, 0.5-2 mm size). Abundant quartz grains were present along with dark grey rock fragments (possibly limestone), angular black fragments of wood/charcoal and particles of ceramic (Figure 5). Under binocular microscopy the sample contained abundant rounded medium to coarse grained quartz grains, dark black angular shiny pieces of charcoal and angular fragments of red/orange ceramics 2-3 mm long. Fine grained quartz-rich sandstone clasts were also present. Three thin sections were prepared from mortar sample WBMT 8076. The mortar was very poorly sorted with coarse aggregate grains between 1 and >2.5 cm intermixed with sand grade aggregate. The largest aggregate grains within the sample were composed of poorly sorted, clay-rich, lithic sandstones. Other clastic lithics present were: mica-rich fine-grained sandstones; micaceous siltstone clasts; quartz-rich sandstones with quartz overgrowth cements post-dated by kaolinite cements; sandstone composed of quartz grains within an Fe oxide "matrix"; quartz dominated sandstone and rare

calcite-cemented quartz sandstones.   Carbonate lithic grains present within this sample included: bioclastic muddy limestones with echinoids, brachiopods, sparry calcite cements, stylolites and minor opaques; recrystallized bioclastic limestones with relict outlines of bioclasts; dolomitised limestone; limestone with pellets and concentrically laminated carbonate grains replaced by Fe oxides. There are brown reaction rims around some of the carbonate lithic grains possibly as a result of firing. Igneous lithic clasts are also present and are dominated by dolerite / basalt. Some of the dolerite grains show alteration to chlorite. Less common aphyric basaltic lithic grains are also present. Sand grade grains (typically fine to coarse sand) within the sample were composed of: monocrystalline and polycrystalline quartz, amphibole/pyroxene and individual bioclasts (bivalves, brachiopods, echinoids). Grains of charcoal are present along with fragments interpreted to be ceramics. The aggregate is intermixed with a lime mortar which has a "mottled" texture with clumps of mortar with different degrees of microporosity / density. The darker "denser" areas have distinctive fracture patterns possibly caused by shrinkage

Sample WBMT 8083 was a pale grey (Munsell 10YR 7/3) sample dominated by coarse angular quartz grains. Aggregate sizes varied considerably, up to a maximum of 50 mm, and were very poorly sorted being composed of large sub rounded sandstones with smaller angular ceramic fragments (Figure 6). The sample was compact and much harder than the other mortars. Thin sections prepared were dominated by a quartz-rich sandstone. Calcite cements are also present within the sandstone. The sample is highly porous with secondary porosity associated with alteration of feldspar and mouldic porosity possibly caused by weathering of the

material prior to sectioning. The lime mortar is of variable appearance with areas of

different porosity.

| Figure 5a. Binocular microscope image of WBMT 8076. Scale bar is 2 mm. | Figure 5b. Representative digital photograph of WBMT 8076 |
| Figure 6a. Binocular microscope image of WBMT 8083 Scale bar is 2 mm. | Figure 6b. Representative digital photograph of WBMT 8083 |

Aggregate grading was carried out after acid dissolution of the binder which notably

dissolves carbonates in the aggregate fraction. A comparison of the grading curves

for the mortar aggregate with the envelopes for Type S sand for mortar (BS 1199) or

Type M sand for concrete (BS 882:1992) demonstrated that the aggregate sizes were

larger than would be expected for a modern sand. WESH 1660 was the closest in

grading to a modern lime mortar whereas over 24% of the aggregate in WBMT 8083

was found to be in excess of 10 mm in size. The size of the coarse aggregate

fragments for 3 of the mortars is such that the Roman material would not be termed a 'mortar' by current standards. The individual aggregate fractions were then analysed under reflected light microscopy. Of note were the high concentration of brick fragments in WESH 1660, and the absence of ceramic materials in the coarser fraction of WESH 1625 (although ceramics were present in the finer fractions). The rounded/sub rounded and likely fluvially sourced aggregates of WBMT 8083 contrasted with the relatively more angular lithic particles of WESH 1625 and WBMT 8076. The observed differences in grading and content indicate the use of different sources for the aggregate fraction of each of the four mortars.

The initial XRD, XRF and FTIR characterisation was undertaken on the fractions manually ground and passing the 300 μm sieve in order to focus on the lime fraction of the mortar rather than the aggregates in order to inform the field sampling of limestone. XRD is only able to detect well-crystallised materials, whereas FTIR can also detect amorphous species; both were used to provide a semi-quantitative assessment of the minerals present. The results (XRD – Table 4, XRF - Table 5, FTIR - Figure 7) highlighted high volumes of (crystalline) silica in this fraction despite the intention to prepare a sample of binder with little or no aggregate present. The magnesium content overall was low and the refined lattice parameters for the calcite phases were all slightly larger than for pure $CaCO_3$, which would suggest that divalent cations other than Mg (possibly Fe) were partially replacing for Ca in the lattice and causing the lattice parameter expansion. The exception of higher MgO content in WBMT 8083 (5.6 wt%) over the other mortars (<2.2 wt%) reflects the presence of dolomite as evidenced by both XRD and FTIR. Small amounts of the clay mineral kaolinite was also detected by FTIR and XRD, with the latter estimating the

highest amount with WESH 1625 at 9 wt% and the lowest with WBMT 8083 and

WBMT 8076 at 4 wt%. The broad spectral kaolinite bands observed in the FTIR

spectra indicate that they are poorly ordered, and identified petrographically as

kaolinite cements within the sandstone clasts in the aggregate.

	WESH 1625	WESH 1660	WBMT 8076	WBMT 8083
Quartz	61%	72%	37%	39%
Calcite	17%	17%	16%	13%
Dolomite	4%			27%
Anorthite ($Ca(Al_2Si_2O_8)$)	9%	6%	44%	16%
Kaolinite $Al_2(Si_2O5)(OH)_4$	9%	5%	4%	4%

Table 4 Semi-quantitative mineral content of the mortar samples by XRD

XRD indicated relatively high amounts (in particular for WBMT 8076) of the calcium

end member of plagioclase feldspar, anorthite, this supports the petrographic study.

The loss on ignition values (LOI) presented in Table 5 were derived from the weight

loss during the preparation of the fused beads for XRF analysis and predominantly

represent the loss of CO_2 from the carbonates, however, H_2O loss from the clay

fraction will also contribute to these values, as will any organic matter or sulfates.

Semi-quantitative chemical data from the SEM-EDX spot analyses identified quartz,

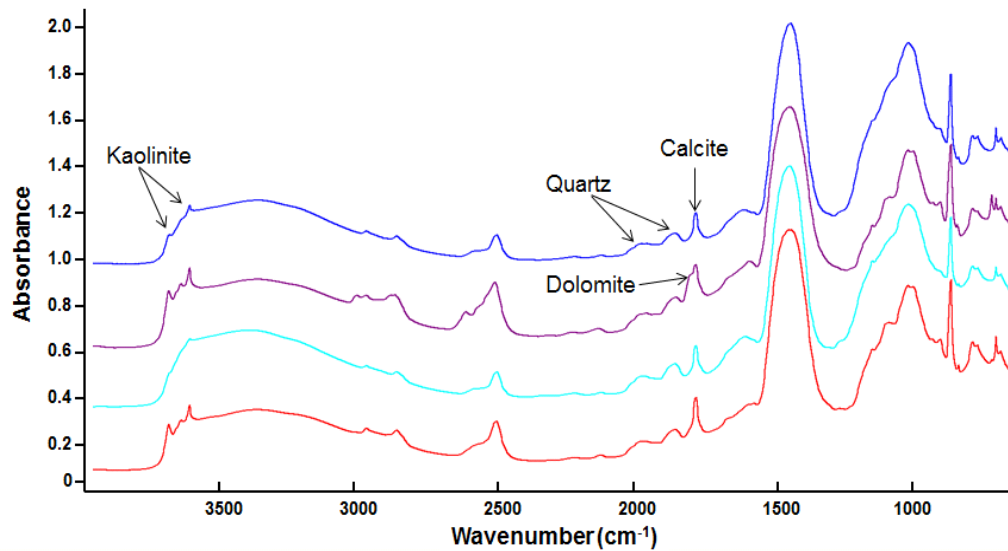alumino-silicate materials (including clays and ceramics) and carbon rich fragments.

Figure 7. Wesh 1625, Wesh 1660, WBMT 8083 and WBMT 8076 (ascending order and offset for clarity)

OXI	LOI:	Na_2O	MgO	Al_2O_3	SiO_2	P_2O_5	SO_3	K_2O	CaO	TiO_2	Fe_2O_3
WESH 1625 S1	22.4	0.3	1.7	4.5	46.4	0.1	0.2	0.7	18.8	0.4	4.3
WESH 1660 S2	17.8	0.0	1.4	7.3	56.6	0.1	0.1	0.9	12.2	0.4	2.9
WBMT 8083 S3	28.9	0.3	5.8	4.2	35.2	0.2	0.3	0.6	19.5	0.4	4.1
WBMT 8076 S4	15.8	0.8	2.2	7.1	52.5	0.2	0.2	0.7	13.2	1.1	5.9

Table 5XRF results from OXI programme on sieved fraction of sample. Mn and Ba results removed

	Dissolution data		
			B/A ratio
	soluble SiO_2	% carbonate	(1:X)*
WESH 1625	2.9	39.5	1.5
WESH 1660	5.5	29.4	2.2
WBMT 8076	6.1	25.8	2.6
WBMT 8083	4.0	31.6	2.0

Table 6 Total soluble silica, % carbonate and binder: aggregate ratio for whole mortar

Dissolution tests were carried out on crushed powder from the mortar as a whole and therefore represents the total soluble silica including that within aggregate particles which would be unable to react with the lime mortar in practice. Figure 8 and Table 6 indicates that for all mortars the levels of soluble silica is relatively low.

Mercury porosimetry of the whole mortars identified higher porosity in WESH 1660 and WBMT 8076 (30.5 and 34.6 % , respectively). WBMT 8076 has the smallest pore diameter average (predominantly 0.1 μm), whereas WESH 1660 has the largest pore diameter average (predominantly 2 μm). WBMT 8083 and WESH 1625 have similar pore size distributions (0.1 and 2 μm) yet have overall lower total porosities (23.8 and 19.9%).

Results of tests on the limestone material from potential sources

Appraisal of the limestone followed similar methods to those used in the evaluation of the mortar and largely follow the schemes illustrated in Figures 1a-c albeit with a focus on the whole rock rather than binder characterisation. Descriptive work began with the recording of the limestone source samples by digital photography (Figure 8a; Figure 8b). The samples were then described and classified in hand specimen as follows.

- A-1 is a medium to dark grey, highly crystalline limestone
- A-2 is a dark grey limestone, crystalline but bioclastic, with brachiopods.
- Sample A-3 is a light grey, fine grained, micritic limestone with crinoidal fragments present.
- Sample A-4 is a light grey, highly crystalline limestone.
- Sample A-5 is a medium grey, compact micritic bioclastic, crystalline limestone. Possible crinoids and gastropods were observed in the hand specimen.
- Sample A-6 is a medium grey, compact, micritic limestone with brachiopods and crinoids present.

- Sample B-1 is a buff yellowy-brown coloured limestone. The sample is crystalline / granular in texture with no preferred fracture planes or bedding.

- Sample B-2 is a medium grey in colour weathering to a brown limestone. The sample is well cemented but highly crystalline in appearance with abundant vuggy porosity.

Petrographic descriptions are summarised in Table 7, with XRD data in Table 8 and FTIR spectra in Figures 9a and 9b, which confirmed identification of two predominantly dolomitic limestones (A-4 the Five Yard Limestone near Housesteads and B1 the Raisby Formation at Trow) whilst the other limestones were predominantly calcitic.

The FTIR spectra of samples A-1 and A-2 are very similar to each other and to that of calcite, confirming that calcite is the dominant mineral present in both samples. The spectra of samples A-3, A-5 and A-6 are also predominantly calcite. There are additional characteristic bands in these spectra at 3695, 3668, 3651 and 3620 cm^{-1}. These bands are a good match to the spectra of kaolinite although their lack of resolution indicates that the kaolinite is of poor order with defects in the crystal structure. Sample A-3 has additional bands at 1987, 1870 and 1112 cm^{-1}, confirming a relatively high amount of quartz. The spectrum of sample A-4 has bands which match those of dolomite as well as bands at 1120, 1035, 1012 and 914 cm^{-1} which indicate the presence of kaolinite. The broad bands between 3000 and 3500 cm^{-1} are probably due to hydroxyl groups associated with kaolinite, but could also be due to other clay minerals like smectites. This band could also be due to the presence of water associated with any minerals present. Sample 1B is dolomite-based, but has less quartz than sample A- 4, Sample B-2 is calcite with minor quartz.
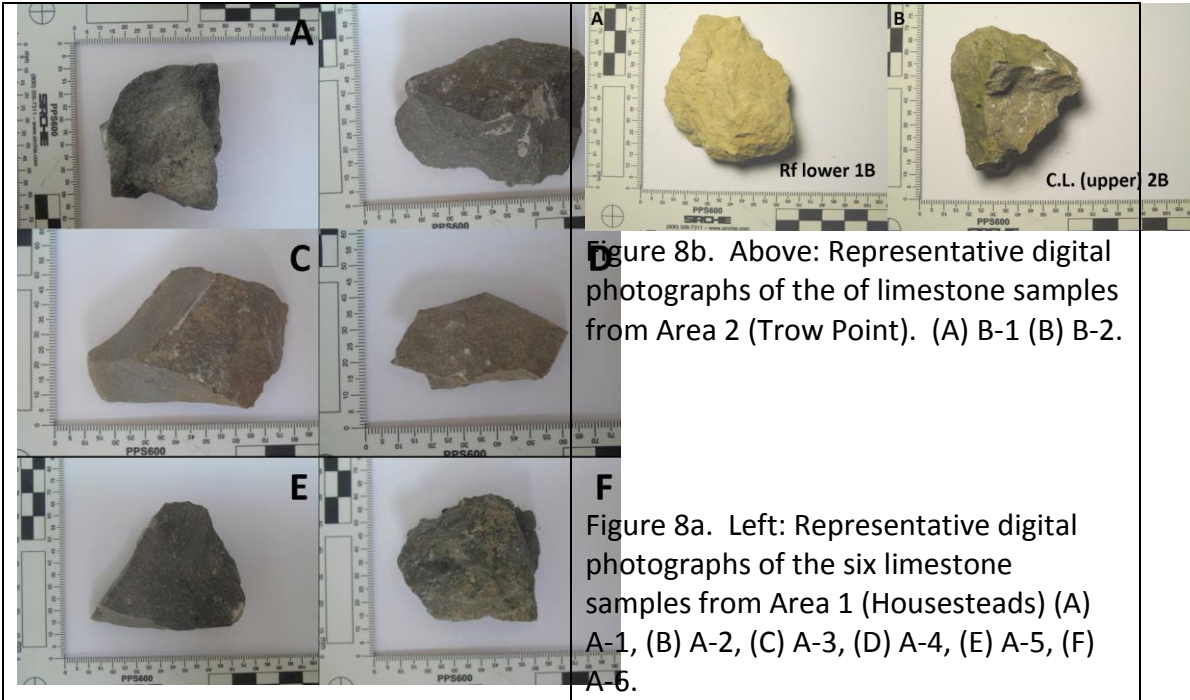
Figure 8b. Above: Representative digital photographs of the of limestone samples from Area 2 (Trow Point). (A) B-1 (B) B-2.

Figure 8a. Left: Representative digital photographs of the six limestone samples from Area 1 (Housesteads) (A) A-1, (B) A-2, (C) A-3, (D) A-4, (E) A-5, (F) A-6.

Table 7. Summary of limestone petrographic characteristics.

Sample	Summary description	Comments
A-1	Recrystalised limestone with sparse relict crinod bioclasts. Interlocking euhedral calcite crystals.	Thermally recrystalised
A-2	Muddy packed bioclastic limestone with abundant foraminifera, crinoids, brachiopods, brachiopod spines, calcispheres, calcareous algae, probably bryozoans, biogenic apatite. Sparry calcite cements minor dolomitisation and rare diagenetic quartz.	Abundant foraminifera rare dolomitisation.
A-3	Bioturbated muddy bioclastic limestone with very abundant elongate spines / spicules, foraminifera, crinoids and gastropods. Sparry to microsparry calcite cements.	Abundant spicules
A-4	Dolomitised limestone with rare echinoid bioclasts retained. Rare quartz cements.	Extensively dolomitised
A-5	Packed bioclastic limestone with abundant brachiopods, calcareous algae, calcispheres, crinoids, foraminifera and probable coral fragments. Micritic matrix with microsparry to sparry calcite cements and calcite syntaxial overgrowths.	Similar to A-2; less abundant foraminifera. Lacks dolomite.
A-6	Muddy packed bioclastic limestone with foraminifera, brachiopods, calcareous algae, bryozoa, trilobites and corals. Sparry calcite and overgrowth cements. Stylolites postdated by minor dolomitisation.	Stylolites post-dated by minor dolomite cements.
B-1 (RF)	Recrystalised limestone with carbonate crystals in a poikilotopic carbonate cement	Dolomitic
B-2 (CL)	Recrystalised dolomitised limestone with extensive vuggy porosity, postdated by sparry calcite cements	

Table 8 XRD Semi quantitative phase analysis for limestones

		Major phase	Minor phase
A-1	Upper Bath House Wood / Scar	Calcite	
A-2	Colwell	Calcite	
A-3	Four Fathom	Calcite (69%)	Quartz (31%).
A-4	Five Yard	Dolomite	Graphite
A-5	Great Limestone	Calcite	Graphite
A-6	Three Yard	Calcite	Graphite
B-1	Raisby Formation	Dolomite (91%)	Ca_2SiO_4 (9%)
B-2	Concretionary Limestone Formation	Calcite (94%)	Quartz (3%) Dolomite (3%)
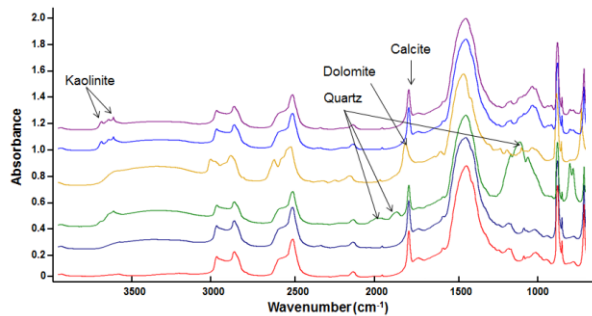
Figure 9a Samples A-1 to A-6 (40ºC dry) - ascending order
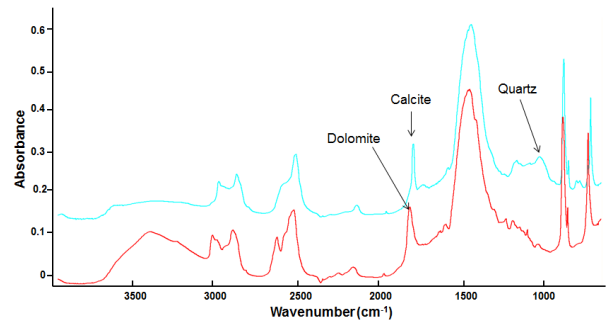
Figure 9b Samples B-1 and B-2 - ascending order

Discussion

The initial investigation attempted to separate the aggregate from the mortar using the common grinding and manual sieving method. The assumption is that the resulting fine fraction will consist of binder and the coarse fraction the aggregate. This was found to be unsuccessful, once the 'aggregate' fraction was analysed, due to the variable nature of the mortar which was friable as a whole but with patches of considerably higher coherence within the aggregate. Aggregates were therefore separated with HCl which dissolved the carbonate lithic fragments seen in the

petrographic analysis and resulted in the observation of aggregate being dominated by clastic siliceous (sandstones / siltstones) along with quartz and feldspar sand size grains. Carbonate lithic grains and individual bioclasts were identified in initial visual characterisation work but were subordinate to the non-carbonate clastic grains which also included a small quantity of igneous grains (dolerite/basalt). With reference to the aggregate in the undissolved mortar, the clastic grains are consistent with having been derived from originally Carboniferous sources, some potentially derived from fluvial sediments originally sourced from Carboniferous bedrock units. Palaeogene micro-gabbro sheets such as the Hebburn dyke, cross-cut the Carboniferous bedrock units in north-east England. The evidence therefore suggests that the aggregates were sourced locally to the point of use. However there are no limestone source rocks at Wallsend to provide a viable feedstock for lime production.

The findings from the analysis of the mortars are broadly in line with the mineral assemblages identified by other authors (Andersen *et al*. 2000; Maravelake-Kalaitzaki *et* al. 2005). Gualtieri *et al*. (2012) discussed the carbonation of brucite $Mg(OH)_2$ which would be formed during processing lime burning with dolomite. This would, they suggest result in amorphous Mg carbonate. As this was not seen in FTIR it suggests that the feedstock was predominantly calcitic. It can be seen therefore that different information is gained from each technique, which is complementary and adds to a fuller characterisation.

The binder to aggregate ratios shown in Table 5 indicate a much richer binder mix for WEST 1625, although the presence of carbonates in the aggregate fraction of the mortar mean that the actual value will be lower than calculated. The findings are in line with those of Böke et al. (2006) at the higher binder end more specifically who found that binder: aggregate volume ratios varied from 1:4 and 1:2. Bartos et al. (2000) proposed that high amount of binder suggests dry slaked air lime, as does the presence of shrinkage cracks or of small zones of fine grained calcite crystals.WESH 1625, 8083 and 1660 have a lower hydraulic character and are therefore more likely to be air limes. Dry slaking is generally associated with lower quality work than wet slaked and matured lime putty. This finding appears to correlate with the identification of charcoal based on microscopy but which was not identified by XRD indicating that it is not well crystallised. The inclusion of these small pieces of charcoal could be indicative of poor management of an intermittent (flare) kiln where the charge had partially collapsed after firing, leading to contamination of the lime with the fuel. If sieving during production was not thorough enough to remove the unburnt charcoal, then it is unlikely to have removed small unburnt fragments of limestone from the lime prior to transportation. Not only could this be indicative of poor quality control but it could also indicate the use of poor quality fuel.

Brick fragments were found by Baronia et al. (1997) in mortars from the latest times of the Roman Empire. Lime mortars with crushed bricks became popular and were also used in the joints of the load-bearing facing walls. Commonly brick clays contain kaolinite ($Al_2O_3.2SiO_2.2H_2O$) and as the clay is fired to around 550°C kaolinite changes to the pseudo hexagonal meta-kaolin ($Al_2O_3.2SiO_2$). If this is present in the

aggregate or as an addition to a lime mortar it reacts, in the presence of water, to

form calcium silicate hydrate ($CaO.2SiO_2.7H_2O$) and tetracalcium alumino hydrate

($4CaO.Al_2O_3.19H_2O$) which give the mortar a hydraulic character (Böke et al. 2006).

The soluble silica content of the mortars is highest for WBMT 8076 and lowest for

WESH 1625. This suggested that the former is likely to have had a degree of

hydraulic set where the latter is more likely to be an air lime. WBMT 8083 and WESH

1660 may also be considered to be feebly hydraulic due to low soluble silica levels.

The lack of reaction halos (for example the extensive rods or fibres of CSH observed

by Bartos et al. (2000)) on the larger ceramic aggregate pieces, suggests that these

imparted no hydraulic properties to the mix and may have been added to provide

dimensional stability to the fresh mortar mix.

With reference to the analysed limestones, evidence suggests that the principle

source of the mortars is unlikely to be the Raisby Formation (B-1) or Five Yard

dolomite (A-4) due to the low levels of magnesium in the mortar. While some

dolomitic grains are present in the aggregate these could have been derived along

with the other lithic content from fluvial sediments.

WBMT 8083 was found by XRF to contain 5.8% of dolomite, which is largely present

in the aggregate fraction. and therefore not linked to the binder source. Fragments

similar to the recrystallized limestone of A-1 (Upper Bath House) were found as small

and rare grains in WESH 1625 which may have been preserved as under-burnt

fragments. While the presence of these grains cannot be entirely discounted from

local aggregate resources, these are more likely to be incorporated into the mortar

along with the quicklime especially when considering that they occur in conjunction

with grains similar to the A-4 (Five Yard dolomite). These outcrops are in places only 100 metres apart and thus both limestone sources could contribute to this mortar. Petrographically similar aggregate grains to limestone sample A-6 (Three Yard) are present in mortar samples WESH 1625 and WBMT 8076 but not in the other two mortar samples analysed. The FTIR and XRD work identified larger amounts of dolomite in WBMT 8083 which were not observed in the petrographic work., probably as this was included in the aggregate content.   Aggregate grains petrographically similar to limestone sample A-5 (Great Limestone) are present in mortar sample WBMT 8076.

The work has indicated that the characteristics of the four mortars are very different and points to divergent sources for both the lime mortar feedstock and the locally derived aggregates. Limestones of similar lithology to those cropping out at Housesteads (and at other areas to the east) were identified in the mortar which was poorly sieved and contained fragments of charcoal. While the presence of fine aggregate grains of petrographically and spectrographically similar characteristics to the rocks at Housesteads is suggestive, the evidence based on this initial work cannot yet be considered compelling when distinguishing poorly burnt lime feedstock present in the mortar rather than added later as aggregate.

There is a common assumption that the lime mortar for the wall was sourced locally along its length. The lime however, was found to more closely match limestone from the west of Housesteads (35 miles to the west of Wallsend) and from the vicinity of the fort at Vindolanda.

This suggests that there was a single source of limestone used when the wall was built (as demonstrated by the sample from the original construction of the baths which can be shown to have taken place at the same time as the curtain was being built at Wallsend – sample WESH 1625). The other three samples are from rebuilding of the baths and curtain in the early to mid-third century, which indicate that the same source could have been operating a century after the work started on the wall. There is a parallel in this suggestion to long-distance transport of lime in Roman Germany. At Iversheim (Sölter, 1970) there was a bank of six large kilns operating in the second and third century. They were operated by the army and the soldier in charge dedicated an altar where he described himself as a magister calcariarum (master of the lime kilns) serving in the 30th Legion which was stationed at Vetera, on the Rhine about 130 km north of Iversheim. Iversheim was identified by isotopic analysis (Berbenni-Rehm, 2005) as one of the sources of the mortar used in the Colonia Ulpia Traiana at Xanten (Germany) although it is approximately 100 km away. Another source for the same buildings was some 66 km distant (Berbenni-Rehm, 2005).

While the Permian limestones around Trow cannot be entirely discounted, the more likely source of the lime mortar would appear to be the Carboniferous limestones near Housesteads. Confining the use of mortar to buildings such as the baths where it was essential and thus reducing the transport of lime over long distances would have speeded up the building of the wall. This fits with recent thinking about the building programme which emphasises that the work was completed as quickly as possible, not least because of the direct involvement of the emperor Hadrian.

Conclusion

Limestones of similar lithology to those cropping out at Housesteads (and at other areas to the east) were identified in the mortar which was poorly sieved and contained charcoal. Confining the use of mortar to buildings such as the baths where it was essential and thus reducing the transport of lime over long distances would have speeded up the building of the wall, which was prioritised after the project was initiated. While the petrographic and spectrographic similarilty of the mortars to the rocks at Housesteads is suggestive as to the source, the evidence based on this initial work cannot yet be considered compelling when distinguishing whether it is derived from poorly burnt lime feedstock present in the mortar rather than added later as aggregate.

Further work is needed to investigate the isotope levels of the mortar from Hadrian's wall and to identify potential limestone feedstocks including two further outcrops near Harlow Hill – the Dalton Limestone (east) and the Newton Limestone (west). Further sampling of mortars from along the line of the wall and associated buildings would build up a larger picture of the mortar chemistry and indicate whether there were significant changes in this over the occupation of the wall. Additionally it is not clear if the coal found in the vicinity of Housesteads was used to augment the local exploitation of timber in lime product during the Roman period. Further work is also needed to consider the possibility that the brick content of some mortars was water worn, which may indicate dredging of material into which building waste had been previously disposed of. Further work on Roman age river sediments and modern river sediments would therefor provide an interesting comparison of the potential aggregate sources.

References

Allison, J (2015) Stone supply to Hadrian's Wall: The western sector reappraised. Unpublished document: Undergraduate Dissertation for Professor I Haynes, Newcastle University

Alvarez JI, Navarro, I, Marin A Garcia Casado, PJ (1999) Methodology and validation of a hot hydrochloric acid attack for the characterisation of ancient mortars. Cement and Concrete Research 29 (1999) 1061-1065 https://doi.org/10.1016/S0008-8846(99)00090-3

Alvarez JI, Navarro, I, Marin A Garcia Casado, PJ (2000a) A study of the ancient mortars in the north tower of Pamplona's San Cernic church. Cement and Concrete Research 30 (2000) 1413-1419 https://doi.org/10.1016/S0008-8846(00)00325-2

Alvarez JI, Navarro, I, Marin A Garcia Casado, PJ (2000b) Thermal, mineralogical and chemical studies of the mortars used in the cathedral of Pamplona (Spain). Thermochimica Acta 365 (2000) 177-187 https://doi.org/10.1016/S0040-6031(00)00624-9

Anderson HD, Zimmermann, Friis H & Shnell, U (2000) Examination of Hydraulic Lime Mortars of Medieval Churches in Denmark. in Bartos, P Groot, C & Hughes JJ (EDS) International RILEM Workshop on Historic Mortars: Characteristics and Tests. Paisley, Scotland 12th-14th May 1999. c RILEM 2000 France:RILEM pp37-42

Baronia G, Binda L, Lombardini N (1997) The role of brick pebbles and dust in conglomerates based on hydrated lime and crushed bricks. Constructuction and Building Materials 11:33–40 https://doi.org/10.1016/S0950-0618(96)00031-1

Bartos, P, Groot, C, Hughes, JJ (2000) PRO 12: International RILEM Workshop on Historic Mortars: Characteristics 459pp

Berbenni-Rehm, C. (2005) Isotope technologies applied to the analysis of ancient Roman mortars:results of the CRAFT project EVK4 CT-2001-30004 Isotopic Technologies applied to Roman Mortars - ITER. Office for Official Publications of the European Communities. January 2005. ISBN: 9789289498838

Bidwell, P (2018) Collapse, demolition & a flooded aqueduct: Hadrian's Wall at Wallsend. British Archaeology July August 2018 pp30-37

Böhm, C (2000) Analysis of Mortars Containing Pozzolanas. in Bartos, P Groot, C & Hughes JJ (EDS) International RILEM Workshop on Historic Mortars: Characteristics and Tests. Paisley, Scotland 12th-14th May 1999. c RILEM 2000 France:RILEM. pp 105-112

Böke, H Akkurt, Sİpekoğlu, B & Uğurlu, E 2006 Characteristics of brick used as aggregate in historic brick-lime mortars and plasters. Cement and Concrete Research 36 (2006) 1115-1122 https://doi.org/10.1016/j.cemconres.2006.03.011

Bowman, A.K. & Thomas, J.D. (1994) The Vindolanda Writing-Tablets *(Tabulae Vindolandenses II)*, British Musem Press, London

Carlton, R Frodsham, P Williams, A. (2011) Northumberland Coast AoNB Limekilns Survey. Journal Name: Archaeology in Northumberland 20 Publication Date: 2011

Coroado J, Paiva, H Velosa, A & Ferreira VM (2010) Characterization of Renders, Joint mortars, and Adobes from Traditional Constructions in Aveiro (Portugal). International Journal of Architectural Heritage. 4 (2) 102-114 https://doi.org/10.1080/15583050903121877

Crow, JG (1991) A review of current research on the turrets and curtain of Hadrian's Wall. Britannia 22 (1991), 56-A3, Society

for the Promotion of Roman Studies http://www.jstor.org/stable/526630

Dix, B (1979) Roman Lime Burning Britannia 10 (1979), 262-A, Society for the Promotion of Roman Studies

http://www.jstor.org/stable/526065

Dix, B (1982) The manufacture of lime and its uses in the western roman provinces. Oxford Journal of Archaeology. Volume 1,

Issue 3, pages 331–346, November 1982 https://doi.org/10.1111/j.1468-0092.1982.tb00318.x

Drdácký, M Fratini, F, Frankeová , D & Slížková, Z (2013) The Roman mortars used in the construction of the Ponte di Augusto

(Narni, Italy) - A comprehensive assessment. Construction and Building Materials 38 (2013) 1117-1128

https://doi.org/10.1016/j.conbuildmat.2012.09.044

Dumayne L (1994) The effect of the Roman occupation of the environment of Hadrian's wall': A pollen diagram from Fozy Moss,

Northumbria. Britannia 25 (1994), 217-224, Society for the Promotion of Roman Studies

http://www.jstor.org/stable/526998

Franquelo, ML, Robador, MD, Ramírez-Valle, V Durán, A Jiménez de Haro, MC & Pérez-Rodríguezm JL (2008) Roman ceramics of

hydraulic mortars used to build the Mithraeum house of Mérida , Spain. Journal of Thermal Analysis and Calorimetry

Vol 92 (21008) 1, 331-335 https://doi.org/10.1007/s10973-007-8810-4

Genestar C, Pons, C & Más, A (2006) Analytical characterisation of ancient mortars from the archaeological Roman city of

Pollentia (Balearic Island, Spain) Analytica Chimica Acta 557 (2006) 372-379

https://doi.org/10.1016/j.aca.2005.10.058

Giles, HL, Hurley, PW, Webster, HWM (1995) Simple approach to the analysis of oxides, silicates and carbonates using x-ray

fluorescence spectrometry. X-ray Spectrometry Vol 24, 205-218 https://doi.org/10.1002/xrs.1300240411

Gillette (2000) Managing a museum 120km long. Museum International 207 V25 n3. 2000 (UNESCO, Paris)

Gualtieri, AF, Romagnoli, M Miselli, P Cannio, M & Gualitieri,AF (2012) Full quantitative phase analysis of hydrated limes using

the Rietveld method. Cement and Concrete Research 36 (2006) 401-406

https://doi.org/10.1016/j.cemconres.2005.02.001

Gulzar, S, Chaudhry, MN & Burg, J (2013) Chemical and mineralogical characterization of old mortars from Jahangir Tomb,

Lahore-Pakistan. Asian Journal of Chemistry Vol 25 No 1 (2013) 133-138

https://doi.org/10.14233/ajchem.2013.14798

Harrison, DJ Hudson, JH & Cannell, B (1990). Appraisal of high-purity limestones in England and Wales. Part 1 resources. British

Geological Survey Technical Report WF/90/16. A report of the Department of the Environment

Hodgson, N (2006) After the Wall - Periods: What is our historical framework fo Hadrian's Wall in the twenty-first

century?Understanding Hadrian's Wall Conference South Shields 3-5 Nov 2006. Arbeia Societry 2008

http://dro.dur.ac.uk/8362/1/8362.pdf

Ingham, JP (2011). Geomaterials under the microscope. Manson Publishing.

Kendal (1996) Transport logistics associated with the building of Hadrian's Wall. Britannia 27 (1996) pp129-152, Society for the

Promotion of Roman Studies http://www.jstor.org/stable/527042

Leone, G, De Vita, A, Magnani, A & Rossi, C (2016) Characterization of archaeological mortars from Herculaniu,. Thermochimica Acta 624 (2016) 86-94 https://doi.org/10.1016/j.tca.2015.12.003

Maravelaki-Kalaitzaki P, Bakolas, A, Karatasios, I & Kilikoglou, V (2005) Hydraulic lime mortars for the restoration of historic masonry in Crete. Cement and Concrete Research 35 1577-1586 https://doi.org/10.1016/j.cemconres.2004.09.001

Maravelaki-Kalaitzaki P, Bakolas, A, Moropoulou, A (2003) Physico-chemical study of Cretan ancient mortars. Cement and Concrete Research 33 (2003) 651-661 https://doi.org/10.1016/S0008-8846(02)01030-X

Middedorf, B Baronio, G & Hughes, J (2000) Chemical-Mineralogical and Physical-Mechanical Investigations of Old Mortars. in Bartos, P Groot, C & Hughes JJ (EDS) International RILEM Workshop on Historic Mortars: Characteristics and Tests. Paisley, Scotland 12th-14th May 1999. c RILEM 2000 France:RILEM pp53-59

Moropoulou, A Bakolas, A & Bisbikou, K (1995) Characterization of ancient, byzantine and later historic mortars by thermal and X-ray diffraction techniques. Thermochimica Acta 269/270 (1995) 779-795 https://doi.org/10.1016/0040-6031(95)02571-5

Moropoulou, A Bakolas, A & Bisbikou, K (2000) Investigation of the technology of historic mortars. Journal of Cultural Heritage 1 (2000) 45-58 https://doi.org/10.1016/S1296-2074(99)00118-1

Özkaya, OA & Böke, H (2009) Properties of Roman bricks and mortars used in Serapis temple in the city of Pergamon. Materials Characterization 60 (2009) 995-1000 https://doi.org/10.1016/j.matchar.2009.04.003

Papayianni, I, Pachta, V & Stefanidou, M (2013) Analysis of ancient mortars and design of compatible repair mortars: The case study of Odeion of the archaeological site of Dion. Construction and Building Materials 40 (2013) 84-92 https://doi.org/10.1016/j.conbuildmat.2012.09.086

Pavia, S., & Caro, S. (2008). An investigation of Roman mortar technology through the petrographic a nalysis of archaeological material. Construction and Building materials, 22, 1807–181. http://hdl.handle.net/2262/64109

Per Lineam Valli (2012) Google Earth overlay, version 1.18. Creative commons http://perlineamvalli.org.uk/about/http://perlineamvalli.org.uk/about/

Pires, J (2014) Simple analysis of historical lime mortar. Journal of Chemical Education (2015) 92, 521-523 https://pubs.acs.org/doi/abs/10.1021/ed500336p

Robador, M.D Perez-Rodriguez, J.L. Duran, A. (2010) Hydraulic structures of the Roman Mithraeum house in Augusta emerita, Spain. Journal of Archaeological Science Volume 37, Issue 10, October 2010, Pages 2426-2432 https://doi.org/10.1016/j.jas.2010.05.003

Šagm, E Böke, H Aras, N & Şerife, Y (2012) Determination of CaCO3 and SiO2 content in the binders of historic lime mortars. Materials and Structures (2012) 45:841-849 http://dx.doi.org/10.1617/s11527-011-9802-1

Silva, DA, Wenk, HR & Monteiro, PJM (2005) Comparative investigation of mortars from Roman Colosseum and cistern. Thermochimica Acta 438 (2005) 35-40 https://doi.org/10.1016/j.tca.2005.03.003

Simpson F. G. (1976) Watermills and Military Works on Hadrian's Wall. Excavations in Northumberland 1907–13. (Edited by Grace Simpson) Kendal: Titus Wilson

Sölter, W (1970) Römische Kalkbrenner im Rheinland. Kunst und Alternum am Rhein. Fuhrer des Rheinischen Landesmuseumns in Bonn herausgegeben im Auftrag des Landschaftsverbandes Rheinland Nr. 31. Rheinland-Verlag GMBH:Dusseldorf

Storemyr, Per(2017) Experimental archaeology: Building a "classic", intermittent limekiln and burning marble at Millstone Park, Hyllestad, Western Norway [online] https://per-storemyr.net/2017/07/13/experimental-archaeology-building-a-classic-intermittent-limekiln-and-burning-marble-at-millstone-park-hyllestad-western-norway/

Symonds M.F.A. & Mason D.J.P Eds (2009). Frontiers of Knowledge. A Research Framework for Hadrian's Wall, Part of the Frontiers of the Roman Empire World Heritage Site. Volume 1 resource assessment. Durham County Council, Durham [online] https://www.dur.ac.uk/resources/archaeology/pdfs/research/Vol_1_Resource_Assessment.pdf {last accessed 29/01/2018]

Thér, R. Maršálek D (2013) Experimental Lime Burning Based on the Findings from the Roman Empire Period. Experimental Archaeology 2013/1 . [online] http://openarchaeology.info/issue-2013-1/ea/experimental-lime-burning-based-findings-roman-empire-period

Velosa, AL, Coroado, J, Veiga, MR & Rocha, F (2007) Characterisation of roman mortars from Conímbriga with respect to their repair. Materials Characterization 58 (2007) 1208-1216 http://dx.doi.org/10.1016/j.matchar.2007.06.017

Yaseen, IAB Al-Amoush, H, Al-Farajat, M & Mayyas, A (2013) Petrography and mineralogy of Roman mortars from buildings of the ancient city of Jerash, Jordan. Construction and Building Materials 38 (2013) 465-471 https://doi.org/10.1016/j.conbuildmat.2012.08.022

Zamba, IC, Stamatakis, MG, Cooper, FA, Themelis, PG & Zambas, CG (2007) Characterization of mortars used for the construction of Saithidai Heroon Podium (1st century AD) in ancient Messene Peloponnesus, Greece. Materials Characterization 58 (2007) 1229-1239 https://doi.org/10.1016/j.matchar.2007.07.004

Acknowledgements